PHYSICAL REVIEW A **70**, 013611 (2004)

Occupation number and fluctuations in the finite-temperature Bose-Hubbard model

L. I. Plimak,[1] M. K. Olsen,[2] and M. Fleischhauer[1]
[1]*Fachbereich Physik, Technische Universität Kaiserslautern, D-67663 Kaiserslautern, Germany*
[2]*Instituto de Física, Universidade Federal Fluminense, Boa Viagem 24210-340, Niterói, Rio de Janeiro, Brazil*
(Received 25 September 2003; revised manuscript received 16 January 2004; published 23 July 2004)

We study the occupation numbers and number fluctuations of ultracold atoms in deep optical lattices for finite-temperatures within the Bose-Hubbard model. Simple analytical expressions for the mean occupation number and number fluctuations are obtained in the weak-hopping regime using an interpolation between results from different perturbation approaches in the Mott-insulator and superfluid phases. With this approach the magnitude of number fluctuations under a wide range of experimental conditions can be estimated and the properties of the finite-temperature phase diagram can be studied. These analytical results are compared to exact one-dimensional numerical calculations using a finite temperature variant of the density-matrix renormalization group (DMRG) method and found to have a high degree of accuracy. We find very good agreement, also in the crossover "thermal" region. We also analyze the influence of finite temperature on the behavior of the system in the vicinity of the zero-temperature phase transition, in one, two, and three dimensions.

DOI: 10.1103/PhysRevA.70.013611 PACS number(s): 05.30.Jp, 03.75.Lm, 03.75.Mn

I. INTRODUCTION

The Bose-Hubbard (BH) model, first studied in the late 1980s [1], has long been considered a rather academic testing ground for analytical as well as numerical approaches in quantum statistical mechanics. Its most interesting feature is the existence of a quantum phase transition [2] at zero temperature between a superfluid and a Mott-insulating phase. With recent advances in the experimental techniques of atom trapping and optical lattices, the BH model has regained substantial practical importance. As noticed in [3], the BH Hamiltonian applies to bosonic atoms trapped in a deep lattice potential. Recent experiments with optical lattices [4] have spectacularly confirmed the existence of the superfluid-insulator transition. Since the Mott-phase is characterized by a well-defined occupation number of the potential wells, the phase transition has important potential applications in quantum information processing [5,6] or Heisenberg-limited matter-wave interferometry [7], both of which require optical lattices with regular filling. Although techniques to eliminate lattice defects have been designed [8], an important issue for the implementation of these applications under experimental conditions are fluctuations in the particle number per site at finite T. In this work we analyze these fluctuations by studying the finite-temperature BH model.

The zero-temperature BH model has been extensively investigated in the past by methods such as the Gutzwiller projection ansatz [9], the strong-coupling expansion [10–13], and Quantum Monte-Carlo [14–18], as well as with various mean-field approaches (see, e.g., [1,19,20]). A very powerful numerical technique in the case of one spatial dimension is the density matrix renormalization group (DMRG) [21], which is used to calculate first- and second-order (i.e., amplitude and number-number) correlations [22]. Less attention has been paid to the nonzero temperature properties of the BH system. We note here that the quantum phase transition exists in the strict sense only at $T=0$. For finite T the compressibility, i.e., the change of the particle number per site with the chemical potential, is always nonzero and thus only an approximate Mott phase exists. Furthermore, the transition between superfluid and insulating behavior passes through an intermediate thermal region. Recently this thermal crossover has been studied within a slave-boson formalism [23]. In this work we study the finite-T properties using a perturbative analytic approach in the strong-coupling limit, deriving simple analytical expressions for the occupation number and number fluctuations that cover both quantum and thermal effects. We are able to verify these results numerically in one spatial dimension by employing a finite-T version of the DMRG approach [21]. We observe good agreement between perturbative and DMRG results, including the description of the thermal crossover between the superfluid and insulating phases. Finally, we analyze the behavior of the BH system in the vicinity of the zero-temperature phase transition in 1D, 2D and 3D, including thermal effects and characteristic scaling behavior in both the superfluid and thermal regions.

II. FINITE-TEMPERATURE NUMBER FLUCTUATIONS IN THE LIMIT OF STRONG CONFINEMENT

We consider a d-dimensional cubic lattice of N nonlinear oscillators characterized by the following Hamiltonian:

$$\hat{\mathcal{H}} - \mu\hat{\mathcal{N}} = \hat{\mathcal{H}}_{\rm hop} + \hat{\mathcal{H}}_0, \tag{1}$$

where μ is the chemical potential, $\hat{\mathcal{N}}=\Sigma_{\boldsymbol{k}}\,\hat{n}_{\boldsymbol{k}}$ is the operator of the total number of atoms, and $\hat{n}_{\boldsymbol{k}}=\hat{a}^\dagger_{\boldsymbol{k}}\hat{a}_{\boldsymbol{k}}$, with $\hat{a}^\dagger_{\boldsymbol{k}}$, $\hat{a}_{\boldsymbol{k}}$ being the usual bosonic creation and annihilation pairs. The lattice sites are numbered with a d-dimensional index $\boldsymbol{k}=\{k_1,\cdots,k_d\}$, while $\Sigma_{\boldsymbol{k}}$ means summation over all lattice sites. The first term,

$$\hat{\mathcal{H}}_{\rm hop} = -J\sum_{\langle \boldsymbol{kl}\rangle}(\hat{a}^\dagger_{\boldsymbol{k}}\hat{a}_{\boldsymbol{l}} + \hat{a}^\dagger_{\boldsymbol{l}}\hat{a}_{\boldsymbol{k}}), \tag{2}$$

on the right-hand-side of (1) is the hopping Hamiltonian, $J\geqslant 0$; the sum extends over nearest neighbors and we assume

cyclic boundary conditions. The second term on the right-hand-side of (1), $\hat{\mathcal{H}}_0=\Sigma_{\boldsymbol{k}} H_{\rm nl}(\hat{n}_{\boldsymbol{k}})$, is a sum of the nonlinear site Hamiltonians

$$H_{\rm nl}(\hat{n}_{\boldsymbol{k}}) = \frac{U}{2}\hat{n}_{\boldsymbol{k}}(\hat{n}_{\boldsymbol{k}}-1) - \mu\hat{n}_{\boldsymbol{k}} = \frac{U}{2}(\hat{n}_{\boldsymbol{k}}-\overline{n})^2 + \text{const}, \quad (3)$$

where $\overline{n}=\mu/U+1/2$ is the filling. The quantum averaging is defined in the standard manner as $\langle\cdots\rangle = Z^{-1}\mathrm{Tr}[\mathrm{e}^{-\beta(\hat{\mathcal{H}}-\mu\hat{\mathcal{N}})}(\cdots)]$, where $Z=\mathrm{Tr}\,\mathrm{e}^{-\beta(\hat{\mathcal{H}}-\mu\hat{\mathcal{N}})}$ is the statistical sum and $\beta=1/T$ is the inverse temperature. Note that oscillator units with $\hbar=k_{\rm B}=1$ are used throughout this paper.

While elaborate methods are needed if we wish to exactly pinpoint lobe boundaries or calculate long-range correlations, local quantities, such as the average number of atoms and the number fluctuations, may be obtained at a lesser cost. We develop such methods separately for the Mott insulator and superfluid phases and then continue by deriving interpolating formulae covering both regions.

A. The Mott insulator

To zero order in the hopping, the ground state of the Mott insulator is $|0\rangle_{J=0}=\Pi_{\boldsymbol{k}}|n_0\rangle_{\boldsymbol{k}}$, where $n_0=\mathrm{round}(\overline{n})$, cf. Eq. (3). A first-order perturbative correction to this state will contain all states that are found from $|0\rangle_{J=0}$ by moving one atom to a neighboring site. All such "single-hop" states are eigenstates of $\mathcal{H}_0$ with the same relative energy U, resulting in an especially simple expression for the ground state to first order in J [24]. Up to second order we find

$$|0\rangle = \alpha\left(\mathbb{1}-\frac{1}{U}\mathcal{H}_{\rm hop}\right)|0\rangle_{J=0} + \mathcal{O}(\mathcal{H}_{\rm hop}^2), \quad (4)$$

where α is a normalization factor. By direct calculation we then find

$$\langle 0|\hat{n}_{\boldsymbol{k}}|0\rangle = n_0,$$

$$\delta n^2 = \langle 0|\hat{n}_{\boldsymbol{k}}^2|0\rangle - \langle 0|\hat{n}_{\boldsymbol{k}}|0\rangle^2 = \frac{2zJ^2n_0(n_0+1)}{U^2}, \quad (5)$$

where $z=2d$ is the number of nearest neighbors in the lattice. These formulas are expected to be a good approximation deep in the Mott-insulator phase, where a large energy gap exists and the thermal occupation of higher levels can be disregarded.

It is worth noting that, if staying within the perturbation approach, these expressions cannot be extended to the thermodynamic limit $N\to\infty$. To demonstrate this, consider the following formula thus obtained for the normalization constant α:

$$\alpha^2\left(1+\frac{1}{U^2}\langle 0|\mathcal{H}_{\rm hop}^2|0\rangle\right)=1,$$

$$\langle 0|\mathcal{H}_{\rm hop}^2|0\rangle = zJ^2Nn_0(n_0+1). \quad (6)$$

These results hold only if $zJ^2Nn_0(n_0+1)\ll U^2$, therefore making the thermodynamic limit impossible. (This problem went unnoticed in Ref. [24].) On the other hand, local (on-site) quantities should become independent of the size of the system when it becomes large enough (thermodynamic limit). In fact, our DMRG simulations show that Eq. (6) equally holds if $zJ^2Nn_0(n_0+1)\gtrsim U^2$.

B. The superfluid

In the superfluid phase, one has to account for states with the total number of quanta different from Nn_0. In the limit of zero hopping, an arbitrary eigenstate is a product state, $|\boldsymbol{n}\rangle=\Pi_{\boldsymbol{k}}|n_{\boldsymbol{k}}\rangle_{\boldsymbol{k}}$. With $\overline{n}$ close to a half integer, it suffices to keep only two states for each site, $|n_0\rangle$ and $|n_0+1\rangle$, effectively turning bosons into fermions [25]. We shall call the subspace of states with $n_k=n_0,n_0+1$, the f-subspace. In this subspace we introduce standard fermionic creation and annihilation operators $\hat{c}_{\boldsymbol{k}}\hat{c}_{\boldsymbol{l}}^\dagger+\hat{c}_{\boldsymbol{l}}^\dagger\hat{c}_{\boldsymbol{k}}=\delta_{\boldsymbol{kl}}$. To make the relation between the bosonic and fermionic states unambiguous, we assume that all sites are enumerated in a particular linear order, and that this order is always maintained when adding "fermions" to the system. For example for a bosonic state with n_0+1 bosons at first two sites and n_0 bosons at all others, $|n_0+1,n_0+1,n_0,\cdots,n_0\rangle=\hat{c}_2^\dagger\hat{c}_1^\dagger|n_0,n_0,n_0,\cdots,n_0\rangle=-\hat{c}_1^\dagger\hat{c}_2^\dagger|n_0,n_0,n_0,\cdots,n_0\rangle$. This eliminates the sign uncertainty emerging from anticommutivity of fermionic operators at different sites. In 1D, it is then straightforward to check that within the f-subspace,

$$\hat{\mathcal{H}}-\mu\hat{\mathcal{N}} = \Delta E\sum_{\boldsymbol{k}}\hat{c}_{\boldsymbol{k}}^\dagger\hat{c}_{\boldsymbol{k}} - J(n_0+1)\sum_{\langle\boldsymbol{kl}\rangle}(\hat{c}_{\boldsymbol{k}}^\dagger\hat{c}_{\boldsymbol{l}}+\hat{c}_{\boldsymbol{l}}^\dagger\hat{c}_{\boldsymbol{k}}) + \text{const}, \quad (7)$$

where $\Delta E=U(1/2+n_0-\overline{n})=Un_0-\mu$. Furthermore, all local (on-site) averages may be reexpressed in fermionic terms by simply replacing $\hat{n}_{\boldsymbol{k}}\to\hat{c}_{\boldsymbol{k}}^\dagger\hat{c}_{\boldsymbol{k}}+n_0$. The latter replacement holds irrespective of dimensionality, this unfortunately being not the case for Eq. (7). The reason is that confining bosons to two local states introduces pseudofermions (spins) rather than fermions proper: we find fermionic (anticommuting) behavior at each site while retaining bosonic (commuting) relations between sites. On the other hand, the distinction between fermions and pseudofermions ceases to be of importance if their density is low. This means that Eq. (7) is exact at the phase transition points, remaining a valid approximation close to these. With this reservation, projection onto the f-subspace makes the Hamiltonian linear so it can be directly diagonalized (omitting the additive constant)

$$\hat{\mathcal{H}}-\mu\hat{\mathcal{N}} = \sum_{\boldsymbol{l}}(E_{\varphi_{l_1}}+\cdots+E_{\varphi_{l_d}})\hat{f}_{\boldsymbol{l}}^\dagger\hat{f}_{\boldsymbol{l}}, \quad (8)$$

where $\boldsymbol{l}=\{l_1,\cdots,l_d\}$, $\varphi_l=2\pi(l-1)/N$, $E_\varphi=\Delta E/d-2J(n_0+1)\cos\varphi$, and $\hat{f}_{\boldsymbol{l}}$ are related to $\hat{c}_{\boldsymbol{k}}$ by a d-dimensional discrete Fourier transform (see Appendix A for details). The average on-site particle number and number fluctuations are then expressed by the average number of fermions per site, $\Delta n=\langle\hat{c}_{\boldsymbol{k}}^\dagger\hat{c}_{\boldsymbol{k}}\rangle$, as

$$\langle\hat{n}_{\boldsymbol{k}}\rangle = n_0+\Delta n,$$

$$\langle\hat{n}_{\boldsymbol{k}}^2\rangle = \langle(n_0+\hat{c}_{\boldsymbol{k}}^\dagger\hat{c}_{\boldsymbol{k}})^2\rangle = n_0^2+(2n_0+1)\Delta n,$$

$$\delta n^2 = \langle \hat{n}_{\mathbf{k}}^2 \rangle - \langle \hat{n}_{\mathbf{k}} \rangle^2 = \Delta n(1 - \Delta n). \quad (9)$$

For Δn we readily find ($\beta = 1/T$)

$$\Delta n = \left(\prod_{s=1}^{d} \int_0^{2\pi} \frac{d\varphi_s}{2\pi} \right) \frac{1}{1 + \exp \beta \sum_{s=1}^{d} E_{\varphi_s}}. \quad (10)$$

This formula holds in the thermodynamic limit $N \to \infty$; in more than 1D, it also implies that either $\Delta n \ll 1$ or $1 - \Delta n \ll 1$.

Interpolating between the insulator and the superfluid

The relations (5), (9), and (10) are found under mutually exclusive conditions. Equation (5) follows if we assume that only the ground state is important and retain the first nonvanishing correction to its wave function; with only one level being important, temperature is of no concern. Conversely, Eqs. (9) and (10) ignore corrections to the eigenstate wavefunctions yet account for energy shifts; with many levels being accounted for, thermal properties are retained. The question we now address is whether a relation can be derived that covers both insulator and superfluid regions, plus, even more importantly, the crossover region (which is naturally termed the thermal region). It would be natural to include perturbative corrections to all "fermionic" states, but this results in some intractable algebra. It turns out, however, that for $J \ll U$, simple interpolating formulas between the two above results may be found that apply not only to the insulator and superfluid regions, but also to the thermal crossover region between them. Namely,

$$\langle \hat{n}_{\mathbf{k}} \rangle = n_0 + \Delta n,$$

$$\delta n^2 = \Delta n(1 - \Delta n) + \frac{2zJ^2(n_0 + \Delta n)(n_0 + \Delta n + 1)}{U^2}, \quad (11)$$

where Δn is given by Eq. (10). The idea behind (11) is relatively simple: for small J, the quantum contribution (5) is negligible in the thermal and (even more so) the superfluid regions, while in the insulator region, $\Delta n \approx 0$ (or 1), so that (11) coincides with (5).

III. RESULTS AND DISCUSSION

A. Comparison with a 1D DMRG calculation

To verify these results in one spatial dimension, we use a finite-temperature version of the DMRG approach [21]. At the core of our approach is the following block-doubling algorithm: assuming that we know the optimized states for a block of length L, we can then find eigenstates of a ring of three such blocks (recall that we use periodic boundary conditions) and calculate the thermal ρ-matrix. Tracing over the states of one block yields the ρ-matrix of a double-sized block. Diagonalizing this ρ-matrix and taking a certain number of eigenstates corresponding to the largest eigenvalues results in the optimized basis for a block of length $2L$. The loss of probability is assessed by summing the neglected eigenvalues; if this loss becomes unacceptable the iterations are stopped. To initiate the algorithm, we start from a ring of $L_0 + L'$ oscillators, and then trace out the states of L' oscillators, resulting in an optimized basis for a block of L_0 sites. We found this to yield much better results than starting from an open-ended block by simply selecting its lowest eigenstates. The full details of the algorithm will be discussed elsewhere.

A word of caution is necessary here. While borrowing much of the technical side of the DMRG method, our approach is conceptually different, the difference residing in the importance of temperature. Similar to other renormalization-group methods, DMRG relies on the fact that the dimension of the physically relevant subspace of the full Hilbert space does not grow with the system size. For finite temperatures this can only be true until the thermal correlation length is reached. Consequently we only grow the block up to a size comparable to the thermal correlation length and must simply stop as soon as the probability loss becomes unacceptable. We use periodic rather than open boundary conditions based on the same argument. For the temperatures considered here, the maximum block length reached in this way is long enough so that finite-size effects are unimportant. For higher temperatures, a combination of stochastic and DMRG techniques can be used, which we are developing and will present in a later work.

The results of our calculations using both DMRG and perturbative approaches in 1D are summarized in Fig. 1, where we plot average on-site numbers and number fluctuations for three cross sections along the μ axis, for $J = 0.01U$, $0.02U$, $0.05U$. Each plot shows data for two temperatures: $T = 0.01U$ and $T = 0.001U$. The top and bottom rows of plots represent, respectively, the on-site population $\langle \hat{n}_k \rangle$ and number fluctuations $\delta n^2 = \langle \hat{n}_k^2 \rangle - \langle \hat{n}_k \rangle^2$. To gain more insight into the thermal region, the middle row of plots shows the difference Δn between the on-site population and the nearest integer value. At $T = 0.001U$, the insulator region is clearly defined by Δn abruptly falling to zero. At $T = 0.01U$, Δn is a smooth function vanishing as μ goes deeper into the insulator region. A similar effect is seen for the on-site number fluctuations. At $T = 0.001U$, the phase transition points are well defined, whereas at $T = 0.01U$ the boundaries of the insulator phase are "eroded" so that δn^2 is a visually smooth function of μ.

Comparing the DMRG to perturbative results, we see that the latter provide a surprisingly good description of the quantities in question. For $J = 0.01U$ (left column of the plots), we find a very good agreement between the perturbative and DMRG results. This agreement is good for $J = 0.02U$ (center column) becoming only fair at $J = 0.05U$ (right column). Note that, even in the latter case, the error is mostly in positioning the thermal region between the insulator and superfluid phases. Away from the thermal region, the results of the perturbative approach show good agreement with the DMRG results, both for the superfluid and for the insulator.

B. Behavior of Δn in the vicinity of zero-temperature phase transition

1. Making Δn computable in 2D and 3D

Equation (10) expresses Δn as a d-dimensional integral, which is of little use in numerics except in 1D. Luckily,

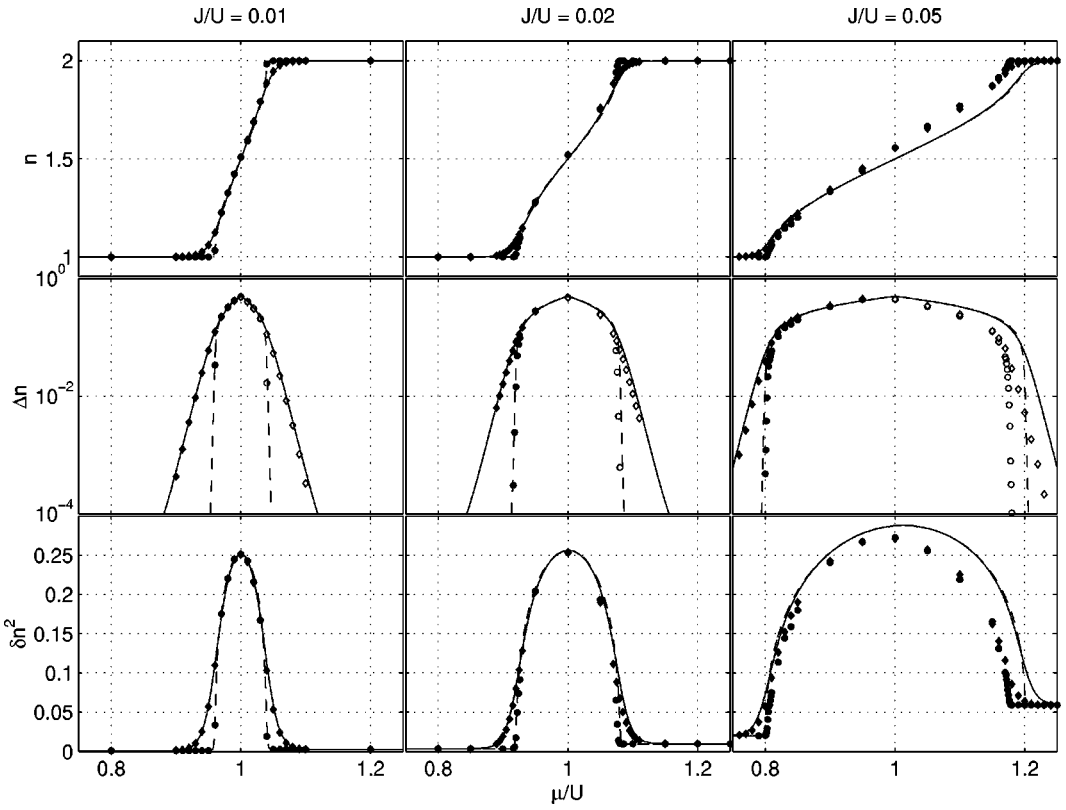

FIG. 1. Average number and number fluctuations versus μ for two temperatures ($T=0.01U, 0.001U$) and three values of the hopping parameter ($J=0.01U, 0.02U, 0.05U$). Top row, on-site population, $n=\langle\hat{n}_k\rangle$; middle row, difference Δn between $\langle\hat{n}\rangle$ and the nearest integer; bottom row, on-site number fluctuations $\delta n^2=\langle\hat{n}_k^2\rangle-\langle\hat{n}_k\rangle^2$. The lines show perturbative results ($T=0.001U$, solid line; $T=0.01U$, dashed line); the markers show results of DMRG calculations ($T=0.001U$, diamonds; $T=0.01U$, circles). Open markers are used for $\Delta n<0$.

irrespective of dimensionality, this integral can be replaced by one that is 1D. As shown in Appendix B,

$$\Delta n = \frac{1}{2} + \mathcal{P}\int_{-\infty}^{+\infty} \frac{dy}{2\pi i} \mathrm{e}^{-iy\Delta E/\sigma} \frac{J_0^d(y)}{\kappa \sinh y/\kappa}, \tag{12}$$

where $\mathcal{P}$ denotes the principal value, J_0 is the Bessel function, $\sigma=2J(n_0+1)$, and $\kappa=\beta\sigma/\pi=2\beta J(n_0+1)/\pi$. Being a Fourier-transform of a singular function, this result is also not quite suitable for numerical use. To remove the singularity, we note that $J_0(0)=1$; adding and subtracting 1 from J_0^d yields:

$$\Delta n = \frac{1}{1+\mathrm{e}^{\beta\Delta E}} + \int_{-\infty}^{+\infty} \frac{dy}{2\pi i} \mathrm{e}^{-iy\Delta E/\sigma} \frac{J_0^d(y)-1}{\kappa \sinh y/\kappa}. \tag{13}$$

The integrand here is a continuous function vanishing exponentially at $y=\pm\infty$, which makes the numerics much easier. Nevertheless, computing this integral for large values of κ remains a challenge. Some details on using relations (12) and (13) as $\kappa\to\infty$ may be found in the appendix.

2. The limit of zero temperature and thermal effects at the phase transition

Having expressed Δn in a computable form, we now wish to derive some analytic approximations. We note that the inital Eq. (10) is more suitable for this purpose than (13). Firstly, consider the limit of zero temperature. As $T\to 0$, the integrand in Eq. (10) turns into a step function, so that

$$\Delta n|_{T=0} = \left(\prod_{s=1}^{d}\int_0^{2\pi}\frac{d\varphi_s}{2\pi}\right)\theta\left(-\sum_{s=1}^{d}E_{\varphi_s}\right). \tag{14}$$

This integral equals 0 unless $|\Delta E|<d\sigma$, or, equivalently,

$$|Un_0-\mu|<2dJ(n_0+1). \tag{15}$$

This condition defines a superfluid "bay" situated between the insulator lobes with the filling factors n_0 and n_0+1. The bay boundaries are at $\mu_\pm=Un_0\pm 2dJ(n_0+1)$. In Fig. 2, we plot the insulator lobe boundaries as predicted by our approach. The insert shows those in 2D found by means of the strong-coupling expansion [11]. Our results are in obvious agreement with the latter, especially for smaller values of J/U. This is also the case for the phase diagrams in 1D as well as in the limit of infinite number of dimensions. (See, e.g., [11] for results of the strong-coupling expansion and Quantum Monte-Carlo.)

At $\mu\approx\mu_-$ (for example), we can use the approximation $\cos\varphi_s\approx 1-\varphi_s^2/2$ in Eq. (14), making the integral, up to a factor, the volume of a d-dimensional sphere. We thus obtain

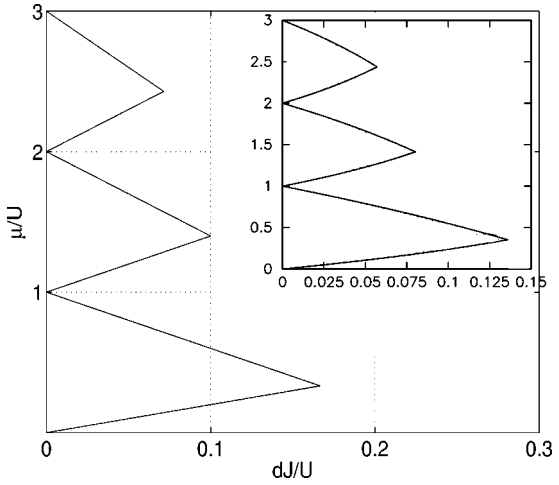

FIG. 2. Phase diagram of the BH model as predicted by our approach. The dimensionless variables dJ/U and μ/U are chosen so as to make the diagram independent of dimensionality (this is an artifact of our approximations). The inset shows the same in 2D found by means of the strong-coupling expansion in Ref. [11]. The scale of the inset matches that of the main graph.

$$\Delta n_{|T=0,\mu\approx\mu_-} = \begin{cases} \dfrac{2}{d\Gamma(d/2)}\left[\dfrac{\mu-\mu_-}{4\pi J(n_0+1)}\right]^{d/2}, & \mu > \mu_-, \\ 0, & \mu \leqslant \mu_-. \end{cases} \tag{16}$$

Figure 3 shows the overall behavior of Δn when μ crosses the superfluid region. The upper plot corresponds to $T=0.001$ ($\kappa=12.73$) and the bottom one to $T=0.01$ ($\kappa=1.273$). Each plot shows Δn as a function of μ in 1D, 2D, and 3D. More specifically, we plot Δn versus a scaled and shifted variable $\xi=\mu/2dJ(n_0+1)-n_0$; the zero temperature phase transition points and the center of the superfuid bay are at $\xi=\pm 1$ and $\xi=0$, respectively. Figure 4 is a blowup of Fig. 3 in a vicinity of the phase transition point at $\xi=-1$. As can be seen from the figures, the overall behavior of Δn as a function of μ changes dramatically, depending on both temperature and dimensionality. At $T=0.001$, the phase transition remains qualitatively defined, as well as the characteristic $(\mu-\mu_-)^{d/2}$ scaling of Δn at the phase-transition point. At $T=0.01$, all these details are washed out. Another observation is that thermal effects are more pronounced for lower dimensionality; e.g., at $T=0.001$, the thermal effects are small except in 1D.

Comparing our results to Ref. [23] we see a number of qualitative as well as quantitative differences. In our approach, the insulator and superfluid phases exist only at zero temperature. At a finite temperature, the superfluid, insulator, and thermal regions are defined only qualitatively. Furthermore, there is no critical temperature of any kind. Thermal effects "switch on" smoothly; strictly speaking, they are not negligible unless the temperature is exactly zero. This appears to be in contrast to Fig. 4 of Ref. [23], which shows a critical temperature for a superfluid-normal phase-transition. Another discrepancy is with, e.g., Fig. 10 of the same work, which shows that the density depends on U for the insulator

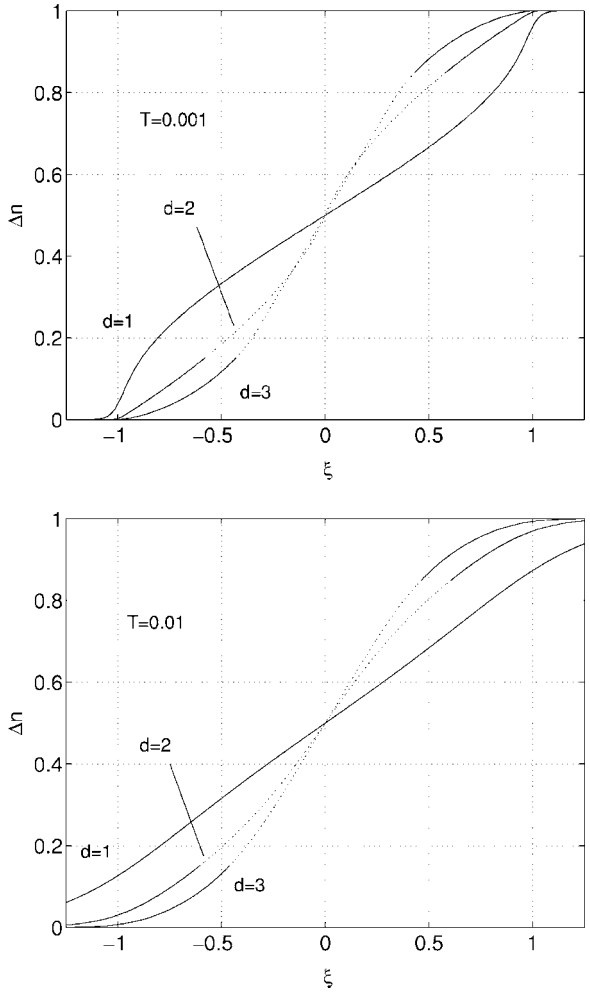

FIG. 3. The overall behavior of Δn as a function of μ, in 1D, 2D, and 3D, for two temperatures: $T=0.001U$ (top) and $T=0.01U$ (bottom). We plot Δn versus a scaled and shifted variable, $\xi=\mu/2dJ(n_0+1)-n_0$; the zero-temperature phase transition points and the center of the superfluid bay are at $\xi=\pm 1$ and $\xi=0$, respectively. For $T=0.01U$, all traces of the phase transition are erased by thermal effects. Change of the line style (solid to dotted) serves to remind the reader that in 2D and 3D our results apply only if Δn is small or close to 1; the same applies to Figs. 4 and 5.

state. Understanding what causes these discrepansies is a subject for further work.

3. The thermal region

Another case when Eq. (10) may be approximated, resulting in additional physical insight, is the "thermal tail" of Δn when μ goes inside an insulator lobe. To be specific, consider the lobe situated below the superfluid bay, with filling n_0, which corresponds to $\mu<\mu_-$. At $T=0$, in this region $\Delta n=0$. If $T\neq 0$, but is large enough, then for $\mu<\mu_-$ we can make the approximation:

$$\frac{1}{1+\exp\beta\sum_{s=1}^{d} E_{\varphi_s}} \approx \exp\left(-\beta\sum_{s=1}^{d} E_{\varphi_s}\right). \tag{17}$$

The integrand being thus factorized, the integral (10) is easily calculated, resulting in

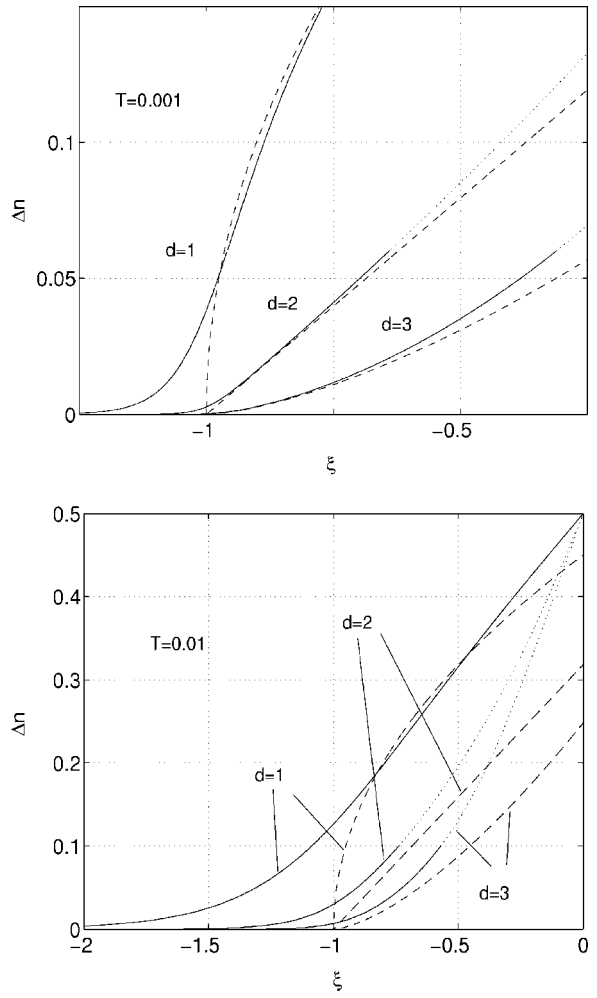

FIG. 4. Δn as a function of μ in the vicinity of the zero-temperature phase transition point, $\xi=-1$. (See the caption to Fig. 3 for more details.) Solid lines are as in Fig. 3; dashed lines represent the zero-temperature approximation $\sim(\mu-\mu_-)^{d/2}$, cf. Eq. (16). The temperature effects decrease with increasing dimensionality.

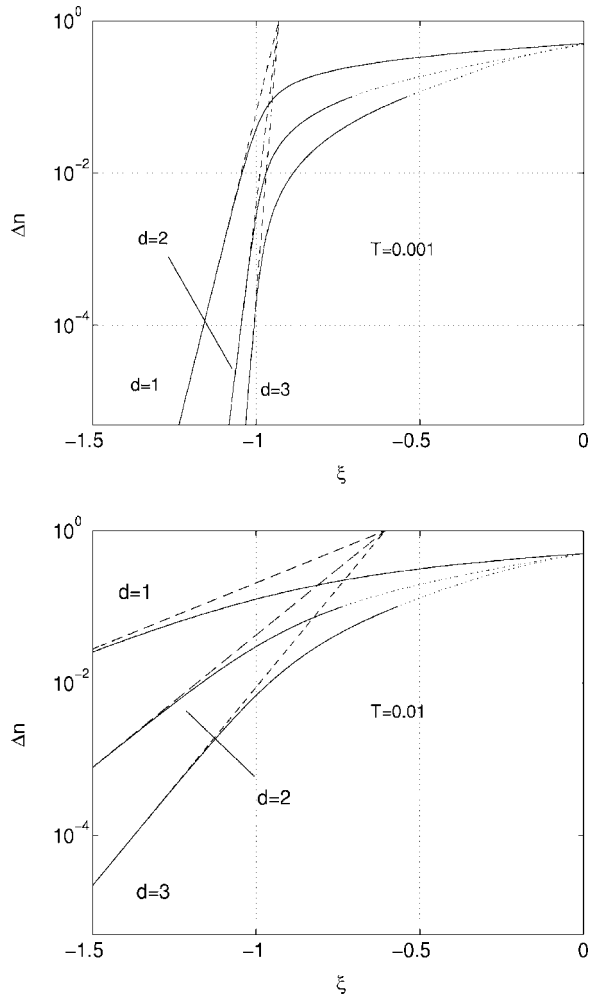

FIG. 5. The "thermal tail" of Δn as a function of μ. Solid lines are as in Fig. 3; dashed lines represent the asymptotic approximation, Eq. (18). The zero-temperature phase transition point is at $\xi=-1$. (See the caption to Fig. 3 for more details.) Note that the "tail" seemingly vanishing faster for larger dimensionality is an artifact of using the scaled variable ξ.

$$\Delta n|_{T\neq 0,\mu<\mu^-} = \mathrm{e}^{-\beta(Un_0-\mu)} J_0^d[2i\beta J(n_0+1)]. \qquad (18)$$

This result is illustrated in Fig. 5 where we plot the results of a direct calculation of Δn, together with the asymptotic relation (18), for the same values of parameters as in Figs. 3 and 4.

IV. SUMMARY

We have developed a simple perturbative approach to the finite-temperature BH model, allowing one to estimate such important quantities as the average number of bosons per site and its fluctuations. This approach gives good results also in the "thermal" region around the (zero-temperature) phase transition point. In 1D, we were able to verify this approach by a finite-temperature version of the density matrix renormalization group technique. A very good agreement was found, especially in the limit of strong confinement.

ACKNOWLEDGMENTS

This research was supported by the Deutsche Forschungsgemeinschaft under Contract No. FL210/12 and the New Zealand Foundation for Research, Science and Technology (Grant No. UFRJ0001).

APPENDIX A: DIAGONALIZING THE HOPPING OPERATOR

We start from writing [cf. Eqs. (2) and (7)],

$$\sum_{\langle \mathbf{kl}\rangle} (\hat{c}_{\boldsymbol{k}}^\dagger \hat{c}_{\boldsymbol{l}} + \hat{c}_{\boldsymbol{l}}^\dagger \hat{c}_{\boldsymbol{k}}) = \sum_{\boldsymbol{k},\boldsymbol{l}} \hat{c}_{\boldsymbol{k}}^\dagger A_{\boldsymbol{kl}}^{(d)} \hat{c}_{\boldsymbol{l}}. \qquad (A1)$$

In 1D, $\mathcal{A}_{kl}^{(1)}=1$ if $k=l\pm 1 (\mathrm{mod}\ N)$, and 0 otherwise. This matrix is diagonalized by the discrete Fourier-transform,

$$\mathcal{U}_{kl} = \frac{1}{\sqrt{N}} \exp\frac{2\pi i(k-1)(l-1)}{N}, \qquad (A2)$$

so that

$$[\mathcal{U}\mathcal{A}^{(1)}\mathcal{U}^{\dagger}]_{kl} = 2\delta_{kl}\cos\frac{2\pi(l-1)}{N}, \tag{A3}$$

and

$$\sum_{\langle \boldsymbol{kl}\rangle}(\hat{c}^{\dagger}_{\boldsymbol{k}}\hat{c}_{\boldsymbol{l}} + \hat{c}^{\dagger}_{\boldsymbol{l}}\hat{c}_{\boldsymbol{k}}) = \sum_{l=1}^{N} 2\hat{f}^{\dagger}_{l}\hat{f}_{l}\cos\frac{2\pi(l-1)}{N}, \tag{A4}$$

where $\hat{f}_l = \Sigma_{k=1}^{N}\mathcal{U}_{lk}\hat{c}_k$. In higher dimensionalities,

$$\mathcal{A}^{(2)} = \mathcal{A}^{(1)}\otimes\mathcal{I} + \mathcal{I}\otimes\mathcal{A}^{(1)},$$

$$\mathcal{A}^{(3)} = \mathcal{A}^{(1)}\otimes\mathcal{I}\otimes\mathcal{I} + \mathcal{I}\otimes\mathcal{A}^{(1)}\otimes\mathcal{I} + \mathcal{I}\otimes\mathcal{I}\otimes\mathcal{A}^{(1)}, \tag{A5}$$

and so on. In dimensionality d the hopping term is diagonalized by the d-dimensional discrete Fourier-transform, $\mathcal{U}^{(d)} = \mathcal{U}\otimes\mathcal{U}\otimes\cdots\otimes\mathcal{U}$ (d times), leading to Eq. (8).

APPENDIX B: EVALUATING EQ. (10) FOR AN ARBITRARY NUMBER OF DIMENSIONS

We rewrite Eq. (10) as [with $\sigma = 2J(n_0+1)$],

$$\Delta n = \int_{-\infty}^{+\infty}\frac{dx}{1+e^{\beta x}}\left(\prod_{s=1}^{d}\int_{0}^{2\pi}\frac{d\varphi_s}{2\pi}\right)\delta\left(x - \Delta E + \sigma\sum_{s=1}^{d}\cos\,\varphi_s\right). \tag{B1}$$

Expressing the Dirac delta in the standard way as a Fourier-transform,

$$\delta\left(x - \Delta E + \sigma\sum_{s=1}^{d}\cos\,\varphi_s\right) = \int_{-\infty}^{+\infty}\frac{dy}{2\pi}e^{iy(x-\Delta E+\sigma\Sigma_{s=1}^{d}\cos\,\varphi_s)}, \tag{B2}$$

allows us to calculate the integrals over the φ's,

$$\int_{0}^{2\pi}\frac{d\varphi_s}{2\pi}e^{iy\sigma\cos\,\varphi_s} = J_0(\sigma y), \tag{B3}$$

where J_0 is the Bessel function. Finally, using the fact that (with $\mathcal{P}$ denoting the principal value),

$$\int_{-\infty}^{+\infty}\frac{dx\;e^{ixy}}{1+e^{\beta x}} = \frac{\pi}{i\beta}\mathcal{P}\frac{1}{\sinh\,\pi y/\beta} + \pi\delta(y), \tag{B4}$$

and with the change of variable $y\to y/\sigma$, we arrive at

$$\Delta n = \frac{1}{2} + \mathcal{P}\int_{-\infty}^{+\infty}\frac{dy}{2\pi i}e^{-iy\Delta E/\sigma}\frac{J_0^d(y)}{\kappa\,\sinh\,y/\kappa}, \tag{B5}$$

where $\kappa = \beta\sigma/\pi = 2\beta J(n_0+1)/\pi$. Furthermore, removing the singularity by adding and subtracting 1 from J_0^d yields

$$\Delta n = \frac{1}{1+e^{\beta\Delta E}} + \int_{-\infty}^{+\infty}\frac{dy}{2\pi i}e^{-iy\Delta E/\sigma}\frac{J_0^d(y)-1}{\kappa\,\sinh\,y/\kappa}. \tag{B6}$$

The integrand here,

$$\frac{J_0^d(y)-1}{\sinh\,y/\kappa}, \tag{B7}$$

is continuous while vanishing exponentially at $y=\pm\infty$.

In the limit of extremely low temperatures, the first term in Eq. (B6) becomes close to a step function. This near-singularity is an artifact and hence has to be compensated by a similar near-singularity in the second term. However, this only affects the calculation of Δn in the vicinity of $\Delta E = 0$. In this region, our results apply only in 1D; Δn around $\Delta E = 0$ is featureless and exhibits very little change with temperature, thus being of no physical interest (cf., Fig. 5). What is important is that, in the vicinity of the phase transition, Eq. (B6) works well for all temperatures, even when $\kappa\to\infty$.

[1] M. P. A. Fisher, Phys. Rev. B **40**, 546 (1989).
[2] Subir Sachdev, *Quantum Phase Transitions* (Cambridge University Press, 1999).
[3] D. Jaksch *et al.*, Phys. Rev. Lett. **81**, 3108 (1998).
[4] M. Greiner *et al.*, Nature (London) **415**, 39 (2002).
[5] Olaf Mandel *et al.*, Phys. Rev. Lett. **91**, 010407 (2003).
[6] D. Jaksch *et al.*, Phys. Rev. Lett. **82**, 1975 (1999); G. Brennen *et al.*, Phys. Rev. Lett. **82**, 1060 (1999).
[7] P. Bouyer, M. A. Kasevich, Phys. Rev. A **56**, R1083 (1997).
[8] P. Rabl *et al.*, Phys. Rev. Lett. **91**, 110403 (2003).
[9] D. S. Rokhsar and B. G. Kotliar, Phys. Rev. B **44**, 10328 (1991).
[10] J. K. Freericks and H. Monien, Europhys. Lett. **26**, 545 (1994).
[11] J. K. Freericks and H. Monien, Phys. Rev. B **53**, 2691 (1996).
[12] N. Elstner and H. Monien, Phys. Rev. B **59**, 12184 (1999).
[13] N. Elstner and H. Monien, e-print cond-mat/9905367.
[14] W. Krauth and N. Trivedi, Europhys. Lett. **14**, 627 (1991).
[15] G. G. Batrouni, R. T. Scalettar, and G. T. Zimanyi, Phys. Rev. Lett. **65**, 1765 (1990).
[16] R. T. Scalettar *et al.*, Phys. Rev. B **51**, 8467 (1995).
[17] G. G. Batrouni *et al.*, Phys. Rev. Lett. **89**, 117203 (2002).
[18] V. A. Kashurnikov, N. V. Prokof'ev, and B. V. Svistunov, Phys. Rev. A **66**, 031601 (2002).
[19] L. Amico and V. Penna, Phys. Rev. Lett. **80**, 2189 (1998); Phys. Rev. B **62**, 1224 (2000).
[20] D. van Oosten, P. van der Straten, H. T. C. Stoof, Phys. Rev. A **63**, 053601 (2001).
[21] S. R. White, Phys. Rev. B **48**, 10345 (1993).
[22] T. D. Kühner, S. R. White, and H. Monien, Phys. Rev. B **61**, 12474 (2000).
[23] D. B. M. Dickerscheid *et al.*, Phys. Rev. A **68**, 043623 (2003).
[24] D. C. Roberts and K. Burnett, Phys. Rev. Lett. **90**, 150401 (2003).
[25] M. Girardeau, J. Math. Phys. **1**, 516 (1960).